Geospatial Analysis of ^{137}Cs in Hiroshima Soil Cores Collected in 1976 and 1978

Harry M. Cullings

Statistics Department, Radiation Effects Research Foundation, 5-2 Hijiyama Park, Minami-ku, Hiroshima 732-0815 Japan

Abstract

In 1976 and 1978 soil samples were collected at a large number of locations in the area of Hiroshima at distances up to 30 km from the hypocenter, to measure radioisotopes such as ^{137}Cs for the purpose of detecting local radioactive fallout from the Hiroshima atomic bomb. The lack of any obvious pattern in these measurements that might correspond to fallout from the Hiroshima bomb has been a source of scientific curiosity over the years. Much has been learned in the past 35 years about the behavior of such radioactive materials in the environment and the interferences caused by worldwide ("global") deposition of radioactive fallout from testing of nuclear weapons in the 1950s and 1960s. However, the analysis of the data from these soil samples, to detect any pattern from the Hiroshima bomb, remains a statistically and analytically challenging problem. We know that the ^{137}Cs in soil from global fallout is large, and it is more recent than any that could remain from the Hiroshima bomb in 1945. Because there are so many variables that affect the retention and migration of the deposited radioactivity in soil, which we presently cannot include in a statistical model, there is a large variation in the measurements from place to place, and it has a spatial structure. To be valid a statistical analysis must consider the resulting "spatial autocorrelation" in the data.

Although an analysis of the data including a careful estimation of the variable effect of long-term rainfall on local deposition of global fallout does not suggest a pattern consistent with local radioactive fallout from the Hiroshima bomb, an important question that remains is how large such a deposition from the Hiroshima bomb would have to have been to be evident in these data. Before an analysis could begin to address the question of how large a deposition of local fallout in 1945 would be detectable in these samples with the interference of global fallout, there is a need to better understand the variables related to soil, terrain and weather that affected the deposition and migration in soil of any radioactivity deposited on the soil surface, and the extent, if any, to which their effect over time on the fallout from the Hiroshima atomic bomb may have been different from their effect on global fallout.

Introduction

For many years there has been concern about the completeness of information in the scientific literature on local radioactive fallout from the Hiroshima atomic bomb, because of the

ISBN 978-4-9905935-0-6
Revisit the Hiroshima A-bomb with Database: 97-124

indications that heavy rainfall ("black rain") shortly after the bombing was concentrated in areas generally to the northwest of the city center (Masuda *et al.* 1989, Uda *et al.* 1953), and because of the relative paucity of early measurements such as area surveys of gamma ray exposure rate in that area, at distances beyond the near range of hills about 2 km from the hypocenter (Okajima *et al.,* 1987). In 1976 investigators took a large number of soil samples (vertical cores) at sites located along rays extending outward from the estimated hypocenter location of the Hiroshima bomb in various horizontal ("compass" or "aximuthal") directions, at 2 km intervals, out to a distance of 30 km at a total of 108 locations (Takeshita *et al.* 1976). These were measured for several fallout-related radioisotopes, most notably ^{137}Cs, but no clear spatial pattern was observed. In 1978 six of these sites were selected to be checked by taking additional samples (Hashizume *et al.* 1978). For each of the six sites, samples were taken at locations closely spaced around the original sampling site from 1976, within a circle about 1.5 km in diameter, and measured. The 1978 samples did not confirm the highest and lowest results from the 1976 samples and suggested that the more extreme results among the 1976 measurements were due to random variation; again there was not any clear indication of the anticipated spatial pattern. In 1985 Yamamoto *et al.* measured aliquots from fourteen of the 1976 samples, primarily for use in isotope ratios that were expected to greatly reduce the variation due to intervening environmental factors affecting original amount of deposition and the fractional retention in the samples of the integrated total of ^{137}Cs that had been deposited at the sampled sites. The results were considered to be consistent with values expected from the worldwide deposition of *global* fallout from atmospheric nuclear weapons testing in the 1950s and 1960s, and no clear pattern of an excess to the northwest was observed. Recently Sakaguchi *et al.* (2010) measured seven new cores of 30 cm's depth in three 10-cm segments each, taken at locations near those of the 1976 samples, for ^{137}Cs and other radioisotopes, thus including measurements of deeper portions of the cores than the top 10 cm portions that were the primary basis of the reported measurements in all of the earlier work. Their conclusions about the ^{137}Cs inventories were similar to those of Yamamoto *et al.* (1985). Whether there is any way to discern a pattern in the data that would correspond to the areas of reported "black rain" or to a plume of local fallout from the Hiroshima bomb in a roughly northwesterly direction has continued to be an unresolved issue.

For several years the author has been interested in this problem and has been engaged in an ongoing attempt to analyze the aggregate of the published data on ^{137}Cs in soil in Hiroshima, to determine what can be learned from statistical methods developed specifically for spatial data, along with stochastic models of the processes affecting the fate of the ^{137}Cs that was originally deposited as either local or global fallout, and other statistical considerations such as the errors involved in the measurements. A major concern in the analysis of these data is the vague nature of the hypothesised area where unmeasured local radioactive fallout is suspected to have occurred. Statistical analyses that are based on comparisons of measured values in two or three areas defined by considerations such as reported rainfall patterns, using general statistical methods such as those for comparing two or multiple samples, are undesirable. By their nature they coarsen the data into two or three spatial categories rather than using the full spatial information in the data, they are dependent on the correctness of the defined areas, and they have other undesirable properties that affect their validity. Rather, the problem calls for statistical methods that have been developed specifically for spatial data (Bivand *et al.* 2008, Cressie 1993). Such methods have been developed extensively over the past 20 to 30 years as a special area in statistics, partly because of the tendency of spatial data to exhibit "spatial autocorrelation": even after the best efforts at modeling the effects of all of the known variables that affect the outcome of interest, it is often found that the adjusted or residual outcome values for locations that are close together are more alike than those for locations that are that are further apart. An important special area of spatial statistics that is *a propos* this problem involves techniques for detection of clustering, hotspots, boundaries and other spatial patterns: in the most recent decade or so, special methods for detecting statistically significant patterns in spatial data, as opposed to those that are likely to have arisen by chance, have been much more extensively developed than before, and many of them have been popularized and made available in software packages (Anselin 1995, Goovaerts and Jacquez 2004, Kulldorff *et al.* 1997, Kulldorff *et al.* 2006, Patil *et al.* 2010). A key property of these methods is that they do not depend on *a priori* assumptions about the locations or sizes of patterns that differ from the assumed background in the data, although some of them detect patterns of a particular shape.

In addition to spatial statistics, there is a need to consider what is known about the total amount of ^{137}Cs that we can expect to have been deposited on the soil surface from global fallout over the years before the samples were taken, and the *soil kinetics* of the deposited ^{137}Cs from both local and global fallout. There is a large variation in measured values at different sites, and this variation must be due to variation in how much total ^{137}Cs was deposited at each site and what happened to that fallout over time due to its *kinetics*; i.e., its motion in the environment due to downward migration in the soil, or its loss from the vertical soil column at the location of deposition due to lateral migration or erosion. Careful calculation from amounts observed at other sites well outside the area of concern in Hiroshima can tell us something about the expected deposition from global fallout. Estimates of long-term rainfall at the various sample locations are particularly valuable in that they can in principle account for most of the spatial variation in the original amounts of ^{137}Cs that were deposited from global fallout. Profiles of the measured concentration of ^{137}Cs vs. vertical depth in soil can tell us something about the kinetics in the vertical direction and possibly about loss from the surface layer due to soil erosion, although not about lateral migration within the soil.

Data

The available data on measured values of ^{137}Cs in soil from the previously described publications are given in the table of the Appendix. Locations are given in Cartesian coordinates with an origin at the estimated location of the Hiroshima hypocenter (Cullings *et al.* 2005). Locations in longitude and latitude and the methods used for estimating them are given in Cullings (2010) and a similarly estimated set of locations for 62 of the samples is available in the HiSoF database (M. Aoyama, personal communication). Measured values have been converted to Bq m^{-2}. Data on monthly and annual rainfall for 157 weather stations throughout Japan are maintained online by the Japan Meteorological Agency, many of them dating back to the 1800s. In addition, starting in 1976 Japan introduced a much larger network of about 1300 automated data collection stations, the AMeDAS system, for which data can be purchased on digital media from the Japan Meteorological Business Support Center.

Analysis

Descriptive Statistics and Sources of Variation

The overall frequency distribution of the measured values from the 1976 study is shown in a histogram in Figure 1. A measured value of 120 Bq m^{-2} for sample 329, located about 26 km due south of the hypocenter, appeared to be a low outlier with different errors than the other data as discussed in previous work (Cullings 2010) and is omitted from the analyses reported here. The left panel in Figure 2 shows the data plotted geographically with the measured values on a color scale. The right panel of Figure 2 shows a smoothed version in which geographically weighted regression (GWR) using the *gw.cov* procedure of the R statistical package *spgwr* (Bivand *et al.* 2008) was used to produce estimates of local means at each location that provide a smoothed set of data. The *gw.cov* procedure was used to calculate a value at each location based on distance-related weighting of the measured values at the 11 nearest neighboring measurement locations (10% of the total number of measured locations). The local variance obtained by *gw.cov* also showed considerable local variation, not shown here. Much of this variation is obvious in Figure 2a, associated with the neighboring high and low values at the ends of rays in the WNW and W directions, but there is also large local variation at the end of the ray in the SE direction. There is also large local variation at the end of the disjointed ray in a roughly NE direction, at least as calculated by the GWR method, but its interpretation must be carefully considered, as it involves two neighboring groups on slightly different lines within each of which there is strong homogeneity.

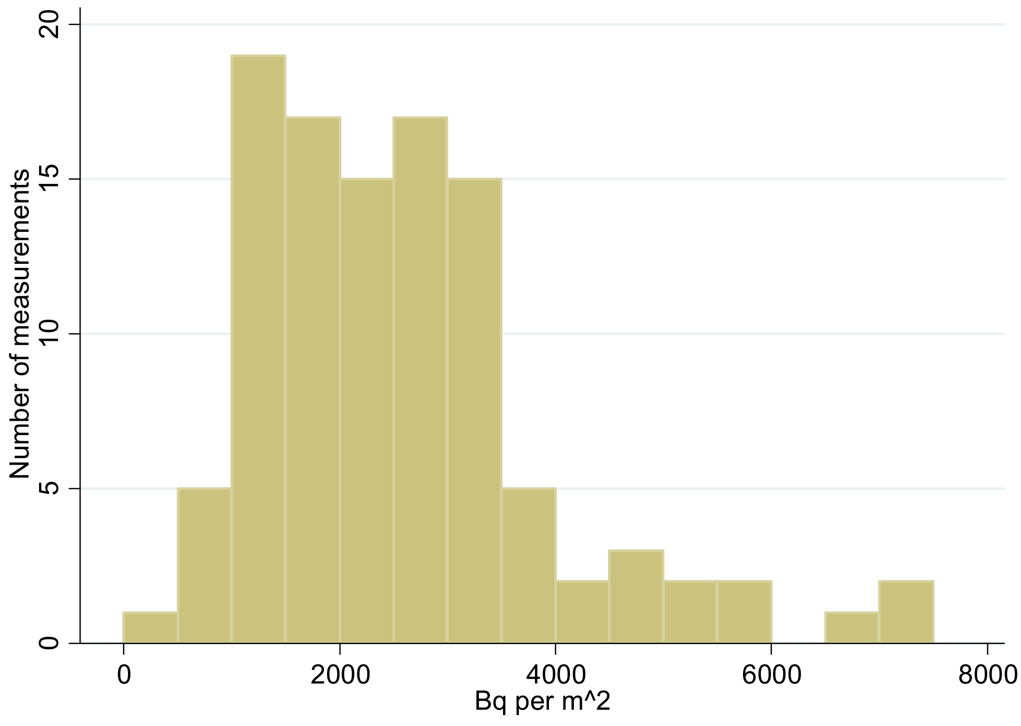

Figure 1 Observed frequency distribution of measured Bq m^{-2}.

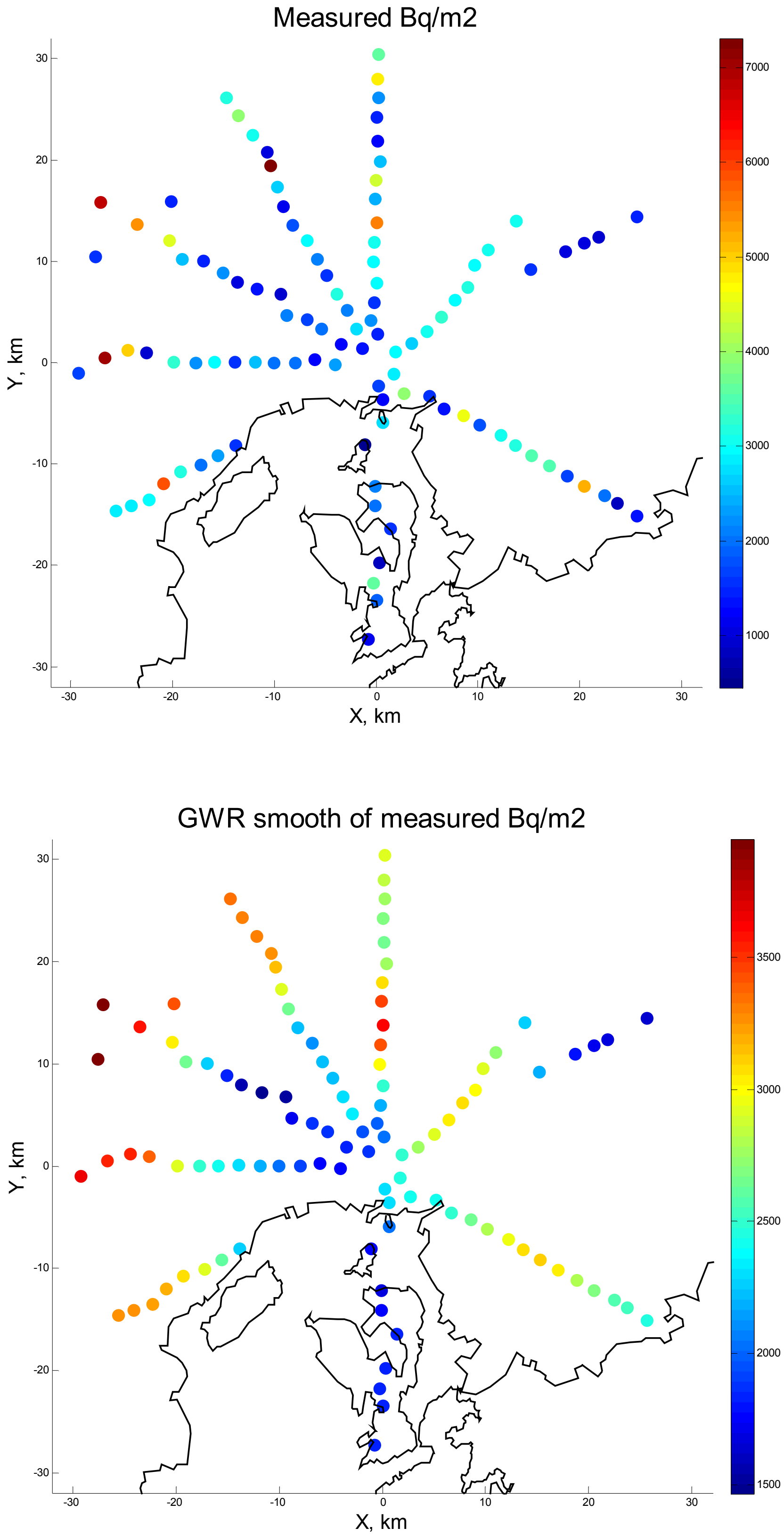

Figure 2 Geographical plots of raw and smoothed measured values of Bq m^{-2} ^{137}Cs.

Variograms

A basic way to evaluate the spatial autocorrelation in data is to estimate variograms. For all pairs of measured values as a function of distance, i.e., $\binom{106}{2} = \frac{106!}{104!2!} = 5512$ possible pairs in this case where 106 measured values are being used, the squared differences measured values in Bq m^{-2}, $(A_i - A_j)^2$, are calculated and partitioned into categories of directed distance $\boldsymbol{h}_{ij}$. The length of $\boldsymbol{h}_{ij}$, $\|\boldsymbol{h}_{ij}\|$, is used for an isotropic variogram that assumes the variogram is equal in all directions, whereas vector forms of $\boldsymbol{h}_{ij}$ are partitioned into categories for directed variograms. The values are then averaged in categories of $\boldsymbol{h}_{ij}$ and smoothed. Directional variograms for four angles are shown in Figure 3, plotted out to distances about twice the usual recommended cutoff, so that it can be seen whether the variogram appears to asypmtotically approach a maximum value. The increase in the variograms at longer distances corresponds to a declining covariance for measured sites that are further apart. This is because the variogram, which we can think of as the variance of the difference between measurements at different sites, is equal to the sum of the variances of the measured values at the two sites minus twice their covariance, under conditions of stationarity, i.e., if the variogram for a given vector separation $\boldsymbol{h}_{ij}$ between two locations does not depend on the locations but only on the distance and direction from one location to the other. There is considerable difference in the appearance of the variograms, which may have to do with aspects of terrain and geography. The spatial autocorrelation appears to be anisotropic, i.e., the covariance declines more rapidly in the directions in the east-west direction than in the north-south direction. In the case of the 90-degree angle (i.e., in an east-west) direction, and possibly other directions, it is not clear that the variogram approaches an asymptote, which is usually called a “sill” in geospatial statistics. This is an indication of non-stationarity in the spatial autocorrelation of the data, i.e., the spatial autocorrelation relationship is not the same in different parts of the study area.

The data show a large variation from place to place: the standard deviation of the logarithms is 0.524, i.e., a coefficient of variation (*cv*; standard deviation divided by mean) of 56% in the original scale of measurement. This variation is due to both 1) measurement error and 2) variation in the actual amount present in soil at the sampled location, but the respective contributions of these two main categories are not clear. In regard to measurement error, it was recognized in earlier work (Cullings 2010) that the estimated variation due to counting statistics was very small compared to the variation among measured locations: except for the omitted sample No. 329, the *cv*s reported by the authors based on counting statistics are < 5%, and therefore counting error does not account for much of the observed variation.

A larger error has to do with using only the top 10 cm of soil, which is the basis for all of the reported values analyzed here except for those of Sakaguchi *et al.* (2010). For the seven cores analyzed by Sakaguchi *et al.* (2010), although we must bear in mind that n = 7 is a very small sample and will not give very accurate estimates, the inventory remaining in the top 10 cm expressed as a proportion of the total inventory remaining in the 30 cm core ranged from 0.71 to 0.96 with a cv of 11%. Another likely basis for substantial error is the processing of the samples and the way in which raw measurement results are used to calculate areal inventory as radioactivity per unit land surface area; e.g., Bq m^{-2}. Of particular concern in this regard is that the soil cores, especially the top 10 cm, are subject to containing considerable amounts of debris, such as pebbles, which are not part of the soil in the sense of being able to contain any of the fallout ^{137}Cs in their interiors, and this needs to be carefully accounted for in calculating areal inventories. Unfortunately, we have very limited data that bear on this and other sources of measurement error.

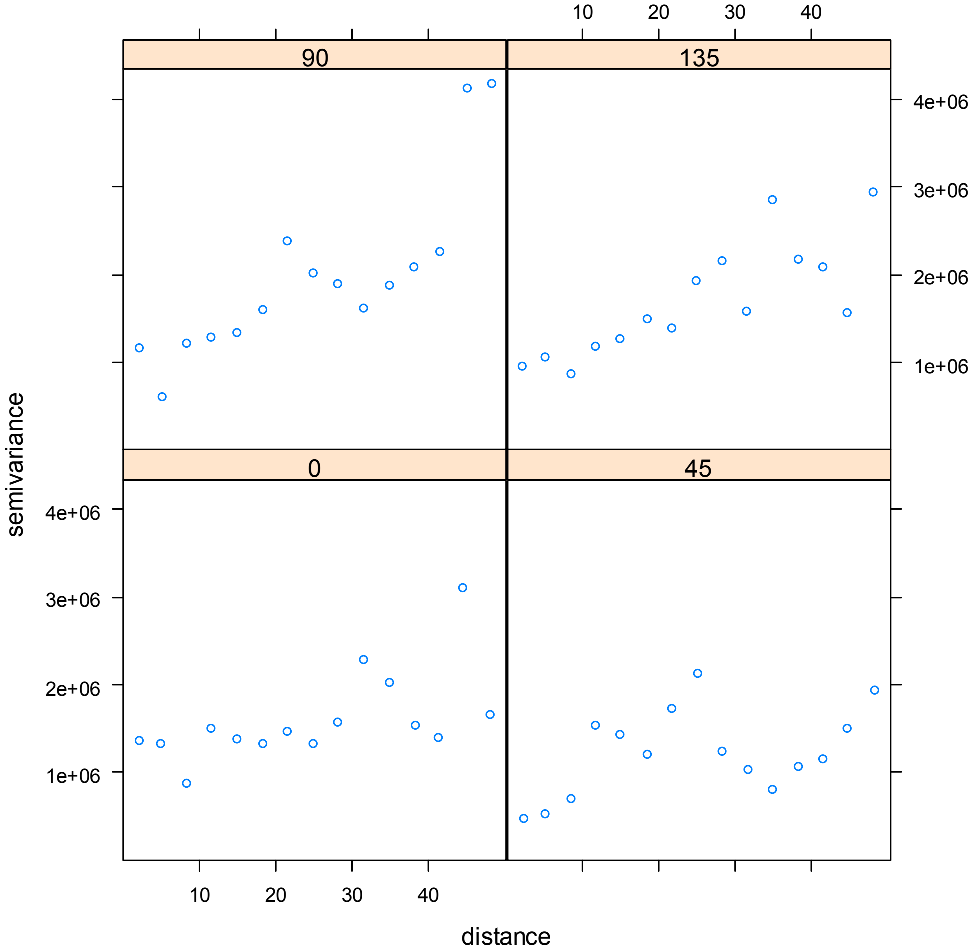

Figure 3 Direction-specific variograms of the raw data: measured Bq m^{-2}.

In summary, we have estimates of counting error from the original work (Takeshita *et al.* 1976), which appear to be trivially small compared to the errors from other sources (Cullings 2010), and we have data from full 30-cm cores (Sakaguchi *et al.* 2010) that give some information on errors from failure to measure the full depth of the core. Apart from these, we have some 14 re-measurements of aliquots of samples from some of the same sites that were measured in 1976, and some 63 samples from 1978 (Hashizume *et al.*) that were taken at locations very close to six of the 1976 locations, all of which can be compared to the original measurements. Unfortunately, in regard to statistical aspects of measurement error, all of the later measurements contain the variation of a potentially different measurement process, particularly in regard to sample preparation and accounting for true soil weight in calculating areal inventories, and all but the measurements of Yamamoto *et al.* (1985) contain some additional spatial variation because they were not from the same exact locations.

In addition to measurement error, there is variation among sites in the kinetics of the ^{137}Cs that was deposited as fallout. A downward movement of the deposited ^{137}Cs into deeper soil occurs by various mechanisms, such as transport processes in the soil water that have a net action similar to diffusion or downward migration, and bioturbation (movement by soil-dwelling organisms). This vertical movement is related to the measurement error described above that is due to measuring radioactivity in only the top 10 cm of soil, as it determines the fraction of the total inventory in a 30 cm core that is below the top 10 cm. In addition, ^{137}Cs can be lost from the top of the soil column due to erosion, and can migrate locally in lateral directions by other mechanisms; these mechanisms of lateral movement or complete removal are ones by which the total inventory in a soil column can fail to reflect the amount that was originally deposited on the soil surface at the sampled location.

Finally, there is a possibility of local variation in amounts of ^{137}Cs that were originally deposited on the soil surface. In the case of local fallout from the Hiroshima bomb, because the nuclear explosion was at an altitude high enough that the fireball did not vaporize and entrain materials from the ground, the deposition occurred in rainfall and not through gravitational settling of larger particles (Okajima *et al.* 1987). Therefore, the variation in local deposition would have been a function of the amount of associated rainfall shortly after the bombing and its locality-specific concentration of ^{137}Cs. This is the pattern for which all of the measurement efforts have been looking. In the case of global fallout, any local variations in original deposition appear more likely to be primarily due to local variations in total rainfall during the years of deposition, primarily in the early 1960s, and not due to local variations in the average concentration of ^{137}Cs in rainwater, $[^{137}\mathrm{Cs}]_{avg}$; as it appears that the latter was fairly uniform over areas the size of the sample grid for this analysis (Aoyama *et al.* 2006). (Based on the quadratic interpolation discussed below, $[^{137}\mathrm{Cs}]_{avg}$ may have differed from the value at the hypocenter by about -1.7% to +1.1% within the sampled area.)

The following sections address several areas in which we have information related to the estimated amount of ^{137}Cs from global fallout and several of the sources of variation in measured values.

Estimates of Deposited Amounts of Global Fallout in Hiroshima and Ishikawa

Aoyama *et al.* (2006) give estimated deposition of global fallout ^{137}Cs as of January 1, 1970, at locations spaced 10° apart in longitude and latitude. Based on an examination of the data and the locations of samples at Hiroshima and Ishikawa that have been measured by Sakaguchi *et al.* (2010), a quadratic interpolation along an appropriate line appeared adequate to give reasonable values for each of those locations. A value of 4754 Bq m^{-2} was obtained for Hiroshima from the data of Aoyama *et al.* (2006) by interpolating values along the 35th parallel of latitude, and a value of 5847 Bq m^{-2} was obtained for Ishikawa by interpolating along a line containing (longitude,latitude) = {(125°,25°), (135°,35°), (145°,45°)}.

Effect of Local Variation in Long-Term Rainfall

Both terrain elevations and elevation gradients were estimated from the contours of detailed 1:2,500 scale maps for the sample locations of Takeshita et al. (1976), which were estimated as described in a previous report (Cullings 2010). Although the dependence of precipitation on terrain is complex, it is well established that at the geographical scale of interest for this work, and particularly for long-term total precipitation, elevation is an important predictor of rainfall (Haiden and Pistotnik 2009, Daly *et al.* 1994). In addition, it is well known that Japan is conventionally divided into three climatic zones with different amounts of rainfall, such that in western Honshu where Hiroshima is located, long term rainfall is highest along the northern coast and decreases to the south (Suzuki 1962). Rainfall in Japan was characterized by Kawachi *et al.* (2001), who used the detailed AMeDAS data to draw an isohyetal map of contours of equal rainfall, although their depictions are too coarse to be useful in this work.

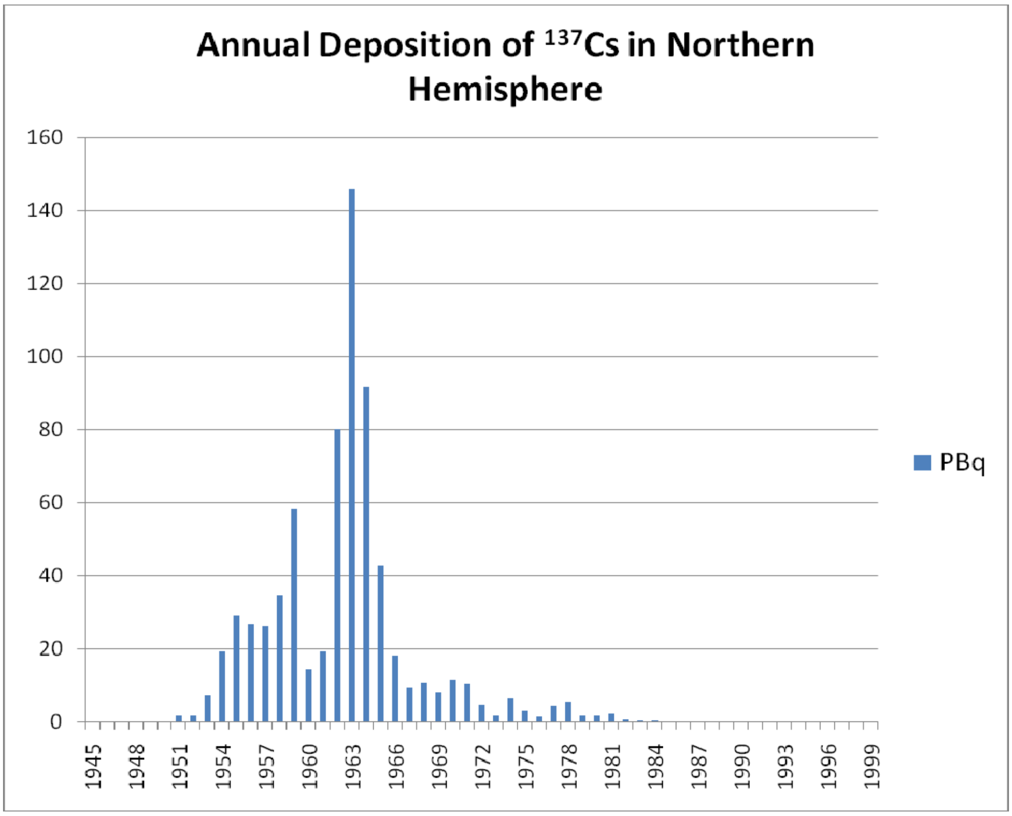

Figure 4 Annual deposition of ^{137}Cs in the northern hemisphere by year, prepared from data taken from UNSCEAR (2000).

Global radioactive fallout was deposited throughout the 1950s through the 1970s, but the vast majority of deposition in the northern hemisphere occurred in the years 1959 and 1962-1964, as shown in Figure 4. A number of major weather stations have online data for all or almost all of these years, but they are confined to coastal locations and provide virtually no information about rainfall in the mountainous interior of Honshuu. To provide a more detailed local model of rainfall, AMeDAS data for the years 1976 through 1995 were obtained and carefully screened to retain only stations and years with complete data. It was found that the number of stations reporting complete years of data increased with time, and a decision had to be made about the tradeoff between temporal and geographical completeness in data selection. A premium was placed on including as many stations as possible within a circle of 50-km radius around Hiroshima, although stations from a substantially wider area were included in the modeling. For the years 1984 plus 1988 through 1995, complete data for stations selected by the above geographical criterion were available. For the same nine years complete data were available for a total of 55 stations between 131.4 and 133.4 decimal degrees east longitude on Honshu and several small, close-lying islands just to the south in the Seto Inland Sea, which were used for modeling. A number of approaches to modeling a trend surface using linear regression were tried with variables including elevation, local elevation gradient and its compass orientation, and a number of geographical variables. The final model selected included elevation and several geographical variables: distance and distance-squared from the northern coast of Honshu, and degrees of longitude east of Hiroshima, taken as 132.4333 degrees east longitude, as shown in Table 1. This produced a good model with an R^2 of 0.816 and residuals whose standard deviation was 7% of the mean value of measured rainfall for the 55 stations. Consideration was given to incorporating additional information from local stations by using simple kriging weights as described in Goovaerts (2000), but it was found that when a variogram was calculated for the residuals from the regression model there was no indication of spatial autocorrelation in them. The measured values for the chosen 9-year period and the modeled values from the regression are shown in geographical plots in Figure 5. The measured values for this 9-year period were within 3% of longer-term averages for the 20-year period from 1976 through 1995, for the large coastal stations with available data: Hamada and Matsue on the north coast of Honshu (and Sakai and Yonago, which are very close to Matsue); and Hiroshima and Kure, which are very close to each other, on the southern coast. For these stations, a weighted average annual rainfall was calculated over an even longer period beginning in 1945, using the ^{137}Cs hemispheric deposition data in Figure 3 as weights. The 9-year averages for 1984 plus 1988-1995 were between 87% and 97% of these weighted averages, suggesting that the years of major deposition were somewhat wetter than average. The spatial pattern among these ratios suggested that the effect on an additive scale was stronger in areas with higher rainfall, i.e., that the effect is roughly multiplicative, but were are not enough major stations to make this a reliable conclusion. A small refinement to the model may be possible by incorporating this information, but was not feasible in the present work.

Table 1 Regression model for annual rainfall.

Source	SS	df	MS		
				Number of obs	55
				F(5, 49)	43.58
Model	3395929.1	5	679185.811	Prob > F	0
Residual	763702.17	49	15585.7586	R-squared	0.8164
				Adj R-squared	0.7977
Total	4159631.2	54	77030.2078	Root MSE	124.84

Parameter	Coefficient	Std. Err.	t	P>t	[95% Conf. Interval]	
altitude	0.6048961	.0835093	7.24	<0.001	0.4370779	0.772714
longH	182.6611	70.63492	2.59	0.013	40.71489	324.6072
Distance_t~t	-2.650002	.6507941	-4.07	<0.001	-3.957822	-1.34218
distnlongH	-13.48773	3.572159	-3.78	<0.001	-20.66625	-6.30921
distnsqlongH	0.0674567	.0327191	2.06	0.045	0.0017052	0.133208
_cons	1763.098	35.26772	49.99	<0.001	1692.225	1833.971

*rain848895 = average annual rainfall for the period 1984 plus 1988 through 1995, altitude in m, longH = longitude in degrees east of 132.4333 degrees east longitude, Distance and distn = distance in km from nearest point on north coast, distnsq = distance^2.

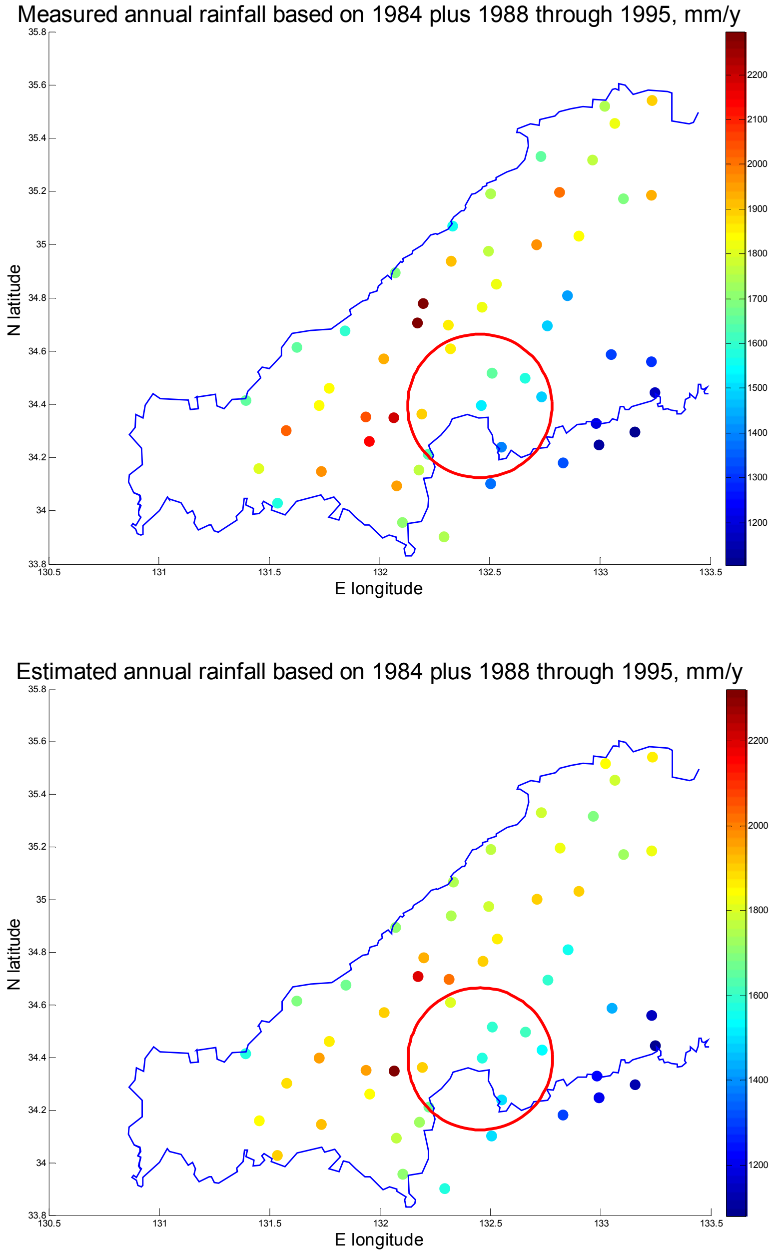

Figure 5 Measured and modeled values of annual average rainfall for a 9-year period in western Honshu. The red circle indicates the area of 30 kms' radius around Hiroshima containing the measured soil samples.

Using the AMeDAS data, rainfall at the Ishikawa location at which soil cores were taken and measured by Sakaguchi *et al.*, for the 9-year period noted above (2010) was estimated at 2475 mm, about 10% higher than their cited estimate of 2200 mm for an unspecified period. Using the value measured in Ishikawa by Sakaguchi *et al.* (2010) with ratios of the modeled rainfall obtained from the regression model for the Hiroshima sample locations, divided by 2475 mm, and multiplying by the activity concentration ratio of ^{137}Cs in rain noted in the previous section, estimated original depositions of global fallout ^{137}Cs a the locations of the measured Hiroshima soil samples were calculated. These values are not plotted here, as they amount to a simple proportional re-scaling of the plot in Figure 5b.

Depth Profiles

Depth profiles of measured [^{137}Cs] in cores provide important information about vertical movement since the original deposition of the ^{137}Cs (He and Walling 1997), and can also provide information about loss due to soil erosion if the erosion occurs by a typical process of laminar removal of the topmost particles of soil (Zhang *et al.* 2008). Several mathematical processes are typically modeled, each of which summarizes the results of a number of actual physical processes, including transport by soil-dwelling organisms (bioturbation). One type of process is a diffusion type, which is conceived as arising from the thermal motion of the material containing the ^{137}Cs at a microscopic level and therefore always maintains a simple monotonic gradient of exponentially decreasing [^{137}Cs] with increasing depth in soil. Another key type of process is often called migration or convection and is thought of as being driven by some active force, even just a downward fluid flow of soil water. The other key process is erosion as described above.

In order to put different profiles on a common basis for comparison and modeling, it may be helpful to plot [^{137}Cs] as a function of cumulative dry mass thickness of soil in units such as g cm^{-2}. This corrects for different soil densities at different levels and in different samples, although it certainly does not correct for the different rate constants that the modeled processes might have in soil layers of different composition. Theoretically, it might be possible to model all three processes in a sample and arrive at some estimate of the original deposited amount of ^{137}Cs, if the core was assayed in thin enough slices and certain restrictive assumptions apply. Practically, however, most investigators have either assumed that erosion (e.g., He and Walling 1997) or migration/convection (e.g., Zhang *et al.* 2009) is negligibly small, which would limit the usefulness of the model for the present problem.

If we use cumulative dry mass thickness to plot the data measured by Sakaguchi *et al.* (2010) for the core from Ishikawa, we obtain the plot in Figure 3. A key feature of this plot is that the maximum is below the top of the core. This can only occur if migration/convection is non-negligible and erosion is negligibly small. The latter is consistent with the authors' observations about the nature of the site. If migration/convection were negligibly small, we might still be able to distinguish whether significant erosion had occurred, by the shape of the plot, as a plot with substantial erosion has a different shape than the pure exponential associated with diffusion alone (Zhang *et al.* 2009).

Figure 6 shows a combined plot of the cores from Hiroshima that were measured by Sakaguchi et al. (2010). Unfortunately, the sections are too thick to allow us to see a realistically small effect of migration/convection that would rule out significant erosion. However, when we look at the plot we can see two types of profiles, which have different mass thicknesses associated with their top 10 cm sections: these are distinguished by solid vs. broken lines in the plot. The fractions of the total core inventory that are in the top 10 cm and the fraction of the estimated original deposition of 5305 Bq m^{-2} that is represented by the total core inventory are given in Table 2.

If we examine the % of the original amount of deposition estimated above that is represented by each core's total inventory (bottom row of Table 2) to either the density of the top 10 cm section (plot) or the shape of the profile as measured by the fraction of the total inventory that is in the top 10 cm (5th row of Table 2), there is somewhat of a trend of increasing total inventory with increasing fraction in the top 10 cm, consistent with the idea that lower fractions in the top 10 cm correspond to loss from soil erosion. However, the sample is small with only 7 cores, and the core at N 28 is highly contrary to the trend. With cores assayed in thinner sections it might be possible to distinguish those with significant loss of inventory due to soil erosion, but this is not certain.

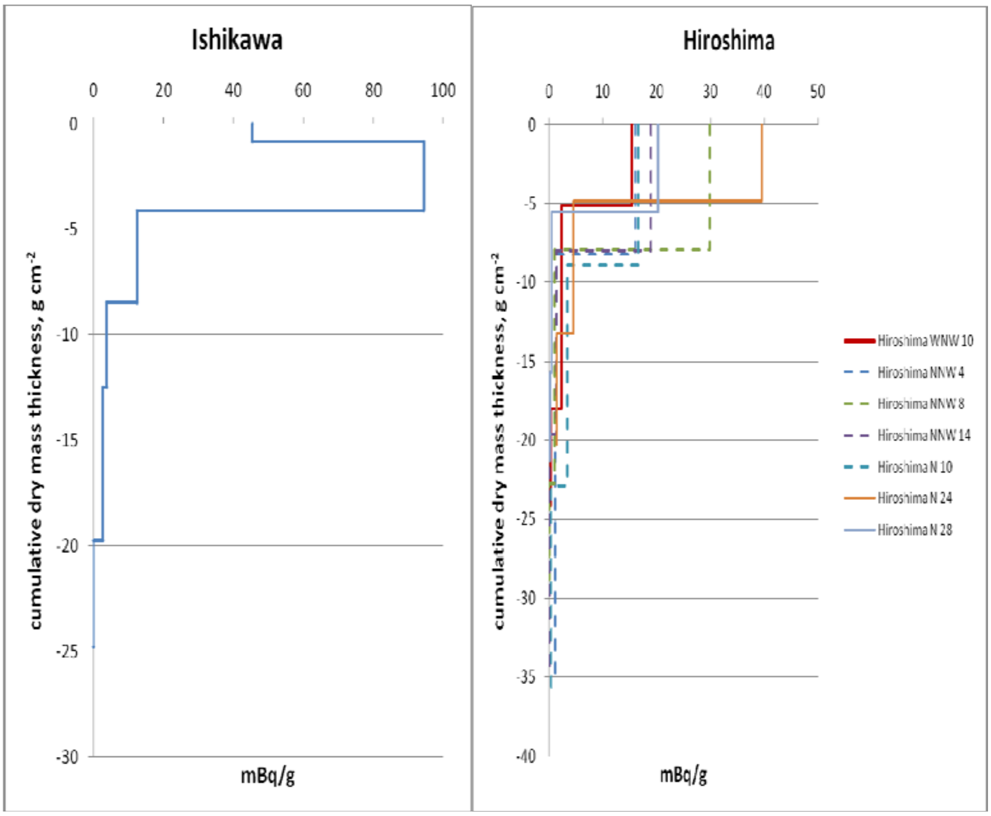

Figure 6 Soil depth profiles of ^{137}Cs in cores from Ishikawa and Hiroshima (Sakaguchi *et al.* 2010).

Table 2 Details of Core Inventories and Relationship to Estimated Original Deposition of Global Fallout in Hiroshima Cores Measured by Sakaguchi *et al.* (2010)

Site	WNW 10	NNW 4	NNW8	NNW 14	N 10	N 24	N 28
Depth, cm	Bq m^{-2}	Bq m^{-2}	Bq m^{-2}	Bq m^{-2}	Bq m^{-2}	Bq m^{-2}	Bq m^{-2}
0 - 10	789	1310	2366	1509	1472	1909	1130
10 - 20	299	174	153	161	474	383	44
20 - 30	19	172	1	5	46	100	7
Total	1107	1656	2520	1675	1992	2392	1181
% in top 10 cm	71	79	94	90	74	80	96
rain, mm/yr	1837	1784	1687	1740	1677	1861	1871
expected Bq m^{-2}	2619	2544	2405	2481	2391	2654	2667
% of expected	42	65	105	68	83	90	44

We should consider the implications of the three processes for statistical analysis. Diffusion and migration/convection do not occur at fast enough rates, regardless of soil type, to carry a significant portion of the originally deposited ^{137}Cs below the bottom of a 30 cm core

(Sakaguchi *et al.* 2010). Therefore they affect the error that is made by measuring only the top 10 cm of soil, but they do not cause an error in the total inventory that is measured for a 30 cm core. Erosion, on the other hand, affects both the fraction of the originally deposited ^{137}Cs that remains in the full core, and the part of that fraction that remains in the top 10 cm. Thus it might be useful to distinguish cores with significant loss due to erosion so that their results could be adjusted or omitted from analyses.

Re-measured areas

The later measurements of Hashiszume *et al.* (1978), Yamamoto *et al.* (1985) and Sakaguchi *et al.* (2010) are informative, but their comparison to the original measurements is somewhat complicated. In the case of Hashizume *et al.* the samples were taken from new locations up to about 1 km from the original sampled locations, partly for the purpose of evaluating local spatial variation, and they are informative in that regard. In the case of Yamamoto *et al.* the samples measured were aliquots of samples originally taken from the locations of the 1976 work; therefore, the local spatial variation is absent and the sources of variation are confined to 1) different true inventories in different cores in the same exact location, 2) effects of aliquoting and sample preparation, and 3) measurement uncertainty; i.e., counting error. In the case of Sakaguchi *et al.* the sampled locations were new locations in the same nominal areas as the original sampling of 1976, so that the sources of variation include a component from local spatial variation in true soil inventories, as in the measurements of Hashizume *et al.* (1978). All of these results have been compared to the original results for the same nominal local areas in a single plot, which is shown in Figure 7.

In the case of the 1978 measurements, we can take the view that the sampling and measurement processes may be comparable for the measurements made in 1976 and 1978, and that we want to see if this is the case, based on the idea that the multiple measurements for each local area in the 1978 data can provide an estimate of the total "within local area" variation in sampling results for both sets of measurements. That is, this would include all the variation due to measurement, sampling, the and variation, within local areas of roughly 1.5 km diameter, in the true values of ^{137}Cs inventory remaining in the top 10 cm of soil. Based on the assumption that the logarithms of the measured ^{137}Cs values are approximately normally distributed, we can use a two-way analysis of variance (ANOVA) for this analysis, with one classification being for local area and the other for year of measurement, where all of the information about the "within local area" variation comes from the 1978 measurements. This gives a marginally significant difference ($p = 0.06$) for 1978 vs. 1976, suggesting that the two sets of measurements may be different. This should not be surprising, because, first of all, the data on neighboring locations are correlated, as will be shown in more detail below. Furthermore,some of the areas chosen for the 1978 measurements were chosen because their 1976 results were particularly high; therefore, they were not likely to be representative of the values that would be expected from repeated measurements in the same areas if the local areas for the 1978 samples had been chosen at random. Consistent with this idea, the standard deviation of the logarithms of the ^{137}Cs measurements from 1976, for the six local areas that were chosen for more sampling in 1978, is 0.59, somewhat larger than the value of 0.51 for the entire set of 1976 measurements, and the mean is higher as well: 7.9 vs. 7.5. Thus there is no statistical evidence that there was anything different about the measurement processes of Hashizume *et al.* (1978) vs. those of Takeshita *et al.* (1976).

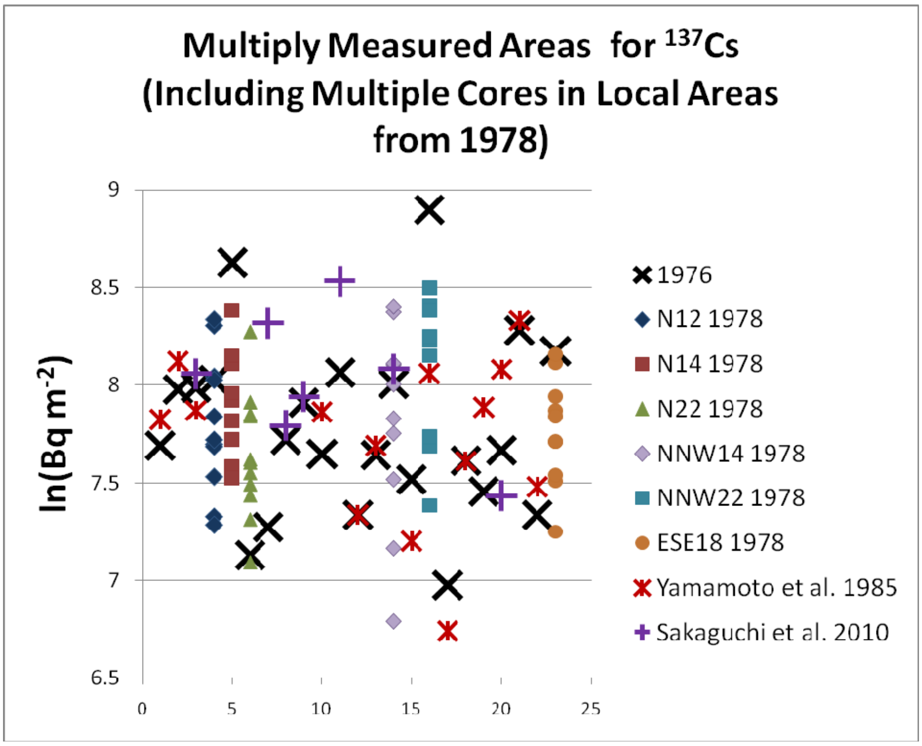

Figure 7 Comparisons among multiple measurements of samples from the same local areas.

We can also compare the results of Yamamoto *et al.* (1985) to the original 1976 measurements of Takeshita *et al.* on samples collected from the same exact locations. For this a simple paired comparison reveals that there is very little apparent difference between the measurement processes of Takeshita *et al.* and Yamamoto *et al.*; the mean difference in logarithms is very small, corresponding to about a 7% difference in the original scale of measurement. As there are no replicates within combinations of site and measurer, we cannot statistically test whether the measurement processes of Takeshita *et al.* and Yamamoto *et al.* are different on samples from the same site, but the mean difference between paired measurements is very small.

Unfortunately, the number of samples measured by Sakaguchi *et al.* (2010) is too small to allow much statistical power for a comparison to the original measurements, especially in light of the fact that the sampling sites, although in the same local area, were not exactly the same as those of Hashizume *et al.* (1976).

Spatial Analysis

The most important first step is to plot the data, which has been done for the raw data in Figure 2. The top panel of Figure 8 shows the ratios of the measured values to the expected values that were calculated using the rainfall model described above. These data were transformed to be normally distributed (Goovaerts and Jacquez 2004) and were smoothed with geographically weighted regression as described above for the raw data. The resulting smoothed data are shown in the bottom panel of Figure 8. This plot provides a visualization in which the relative high and low values can be better compared because the scale is not determined by a few extreme values. This plot summarizes a key result, and it clearly shows where the higher values occur after correction for the effect of rainfall on deposition of global fallout.

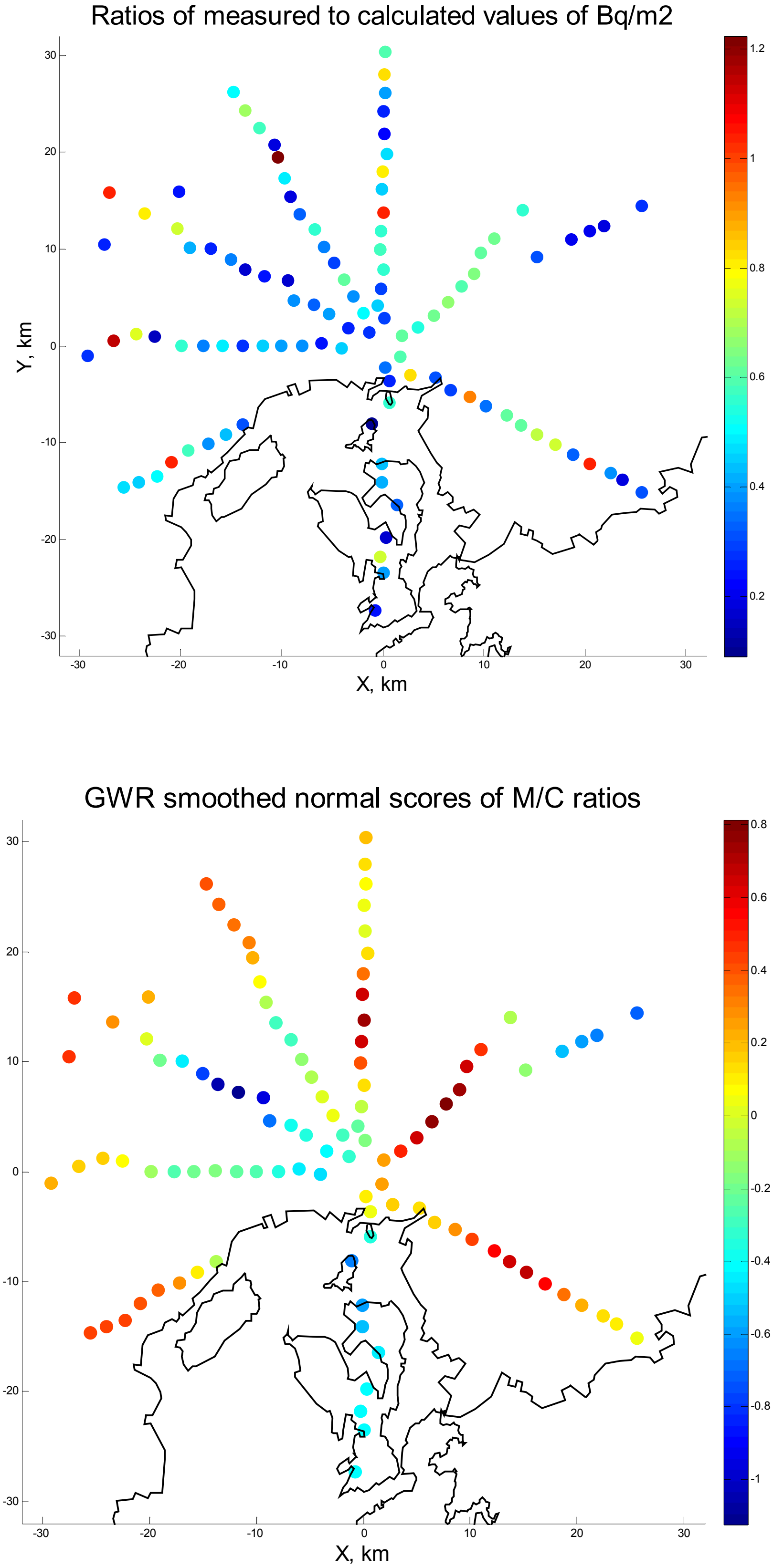

Figure 8 Measured/calculated ratios and GWR-smoothed normal scores.

The LISA statistic and spatial neutral models

In order to evaluate the statistical significance of the ratios of measured to calculated values, a variogram was calculated and fitted for the normal scores. At longer distances around 27 km, the range of the fitted variance function, the variogram appears to level off – this is called the "sill" of the variogram and corresponds to the distance at which the covariance becomes very small and the variogram approaches the sum of the variances of the measurements at the two locations. A spherical covariance function $c(i,j) = psill \times \left\{ 1 - \left[1.5\frac{h(i,j)}{range} - 0.5\left(\frac{h(i,j)}{range}\right)^3 \right] \right\}$, wherein the partial sill "*psill*" is the difference between the sill and the Y-intercept ("nugget") of the semivariance depicted in Figure 9, was fitted to the variogram as shown in Figure 9. Then a local indicator of spatial association (LISA) statistic (Anselin 1995, Goovaerts and Jacquez 2004) was calculated for the normal score of each measured value by using the normal scores of neighboring measurements within a radius of 7 km. This was the minimum radius for which every measurement has at least three neighbors; some have as many as 22 neighbors. For this work the statistic was calculated simply as $LISA_i = Y_i \times \frac{1}{n_J}\sum_{j \in J} Y_j$ wherein J denotes the n_J neighboring measured locations that are within 7 km of the i^{th} location and Y_i is the normal score of the measured value at the i^{th} location. High values of the LISA statistic correspond to values that are large and surrounded by neighbors that are similarly large, or small and surrounded by surrounded by neighbors that are similarly small, whereas small values of the LISA statistic identify locations for which the measured value is larger or smaller than the neighboring values. Thus, high values of LISA identify potential hot *or cold* spots and low values of LISA identify spatially isolated outliers. To evaluate the statistical significance of the LISA statistics, distributions of values were generated by Monte Carlo simulation under two spatial neutral models as described by Goovaerts and Jacquez (2004). In the Type I model, complete spatial randomness of the measured values is assumed, whereas under the Type II model it is assumed as a null hypothesis that the measured values have a spatial autocorrelation as characterized by the covariance model fitted to the variogram as described above, but that they have no particular pattern. In the Type I model, simulated values are generated by simple random spatial permutation of observed values, whereas in the Type II model, simulated values are generated by choosing a random sequence of locations and then generating a value at each location by a random draw from a normal distribution whose parameters are determined by simple kriging weights applied to the normal scores of locations previously generated in the sequence. The parameters for each normal distribution were taken as $\mu = \sum_{k:h(i,k)<range} \lambda_{ik} Y_k$ and $\sigma^2 = (psill + nugget) - \sum_{k:h(i,k)<range} \lambda_{ik} c(i,k)$. The simple kriging weights λ_{ik} were calculated as $\lambda_{ik} = \mathbf{v}'\mathbf{V}^{-1}$, wherein **v** is the vector of covariances $c(i,k)$ between the ith location, which is being simulated, and the kth of the neighboring locations previously simulated that are within the variogram range 27 km of the location being simulated, and **V** is the variance-covariance matrix of the neighboring locations previously simulated that are within the variogram range 27 km of the location being simulated. It was confirmed that these parameters preserved the sample histogram (frequency distribution of the normal scores of the measured values) and provided the

indicated spatial autocorrelation, although of course the variograms of the simulated data were quite variable and many were not amenable to being fitted with a spherical covariance function. A better and more general description of spatial neutral models is given by Goovaerts and Jacquez (2004). These procedures generate realizations specific to each measured location that take into account the number and proximity of its neighbors, and the rank of the LISA statistic of a given measured location, within 999 simulated values for the same location, was used to evaluate statistical significance. The Type II neutral model generated simulated values with wider distributions of LISA statistics than the Type I model consistent with principle, but even for the Type I model, when a Bonferroni correction was applied to the critical value of 0.05, based on the average number of neighbors within 7 km for each measured location, there were no statistically significant values of LISA. The Monte Carlo ranks of the LISA statistics for the Type II model, which is more realistic for these data, are shown in Figure 10. Again, it should be borne in mind that *high* values of LISA relate to contiguous areas of high *or low* neighboring measurements, and *low* values of LISA relate to spatially isolated cases of especially high or low values.

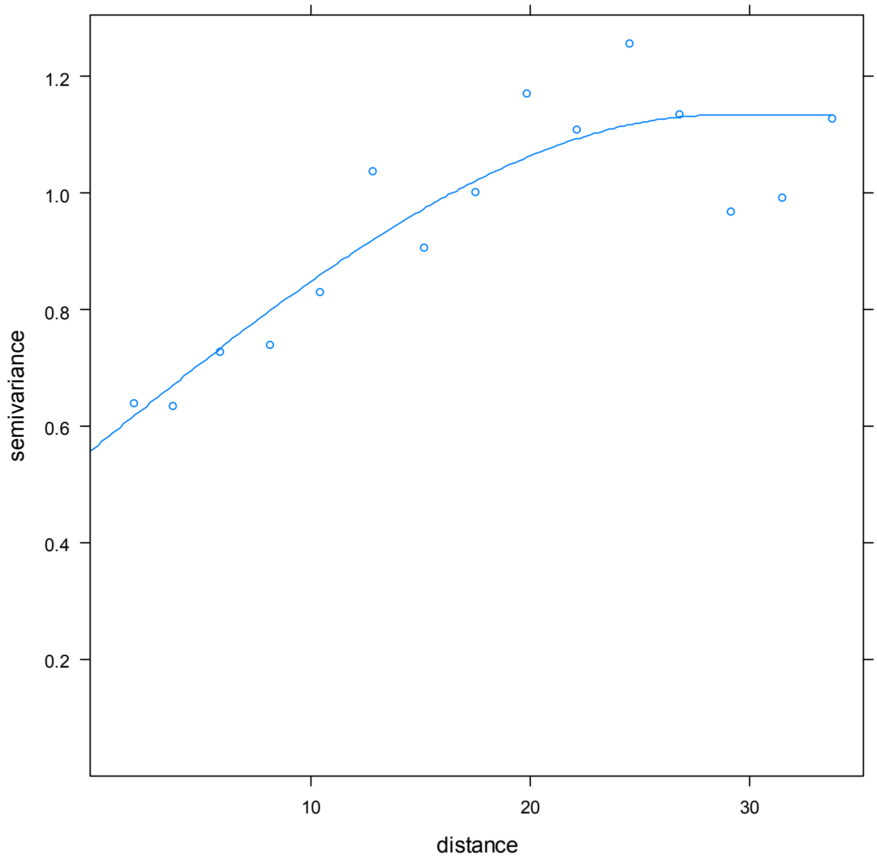

Figure 9 Variogram of the M/C ratios.

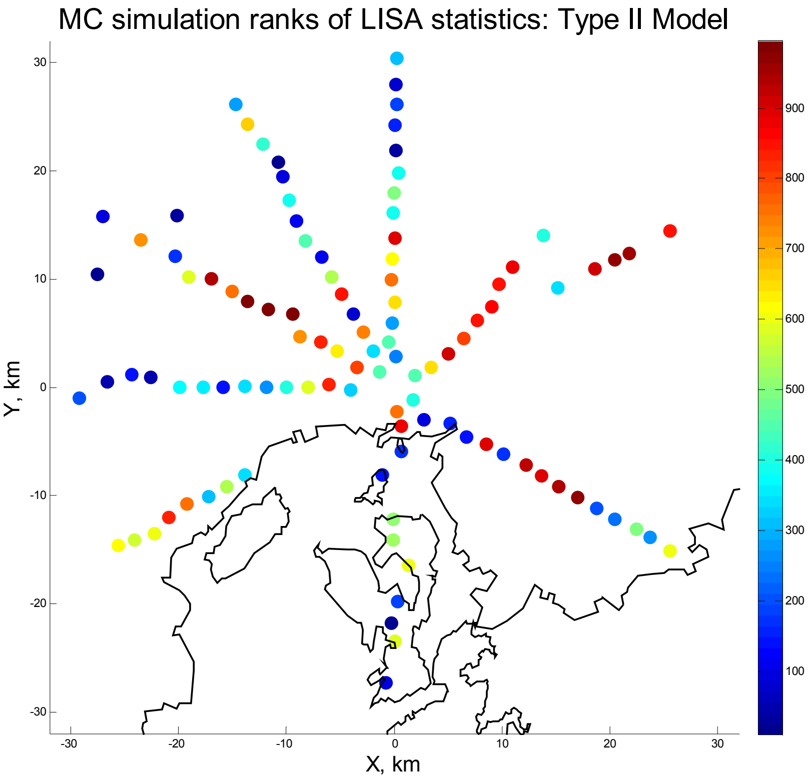

Figure 10 MC simulation ranks (999 simulated sets of data) of LISA statistics for the normal scores of M/C ratios.

Potential for Stochastic Modeling of the Data

The negative result reported here is qualified by the observation that the remaining measureable ^{137}Cs in soil in 1976 would have been greatly obscured by accumulated global fallout as described in detail above. Any method for detecting a pattern that might be attributable to fallout from the Hiroshima bomb would need to be evaluated by stochastic modeling to determine its likelihood of making errors, both false positive and false negative. The first type of error is quantified by the probability that a detection method would give false positive results when there is no fallout present from the Hiroshima bomb, i.e., due to patterns in the inventory of ^{137}Cs from global fallout that arise because of factors that 1) cause spatial nonuniformity of the deposition of global fallout or that 2) affect its movement in the environment, that have spatial structure (i.e., are not constant over the spatial region of interest) and that are not accounted for in the model used for the detection method. The second type of error, false negative error, is quantified by the probability that a signal of a given size from the Hiroshima bomb would *not* be detected by the method in question, in the presence of variable signal from global fallout. As is often the case, the analysis presented here controls better for the first type of error than the second.

Unfortunately, some parts of the stochastic modeling problem are tractable in the present state of knowledge as summarized in the preceding discussion, and others are not. The first thing to consider is the problem of modeling global fallout alone. There are at least two things that need to be considered in this regard. The first is that even after careful estimation of the expected original deposition of global fallout based on modeled rainfall, there appear to be patterns on a fairly large spatial scale, as suggested by the apparent trend in the smoothednormal scores of the M/C ratios, in the mean of the spatial process. The process that gives rise to this, which presumably involves spatially varying attributes of sample locations that affected the retention and migration of the deposited fallout, cannot be modeled with the currently available data.

In addition, there is the problem of creating a useful stochastic model for the original deposition of fallout from the Hiroshima bomb that we would want to be able to detect. The main problem in this regard is that it is still not completely clear how much of the observed variation in the data at hand would affect the signal from the Hiroshima bomb. The effect on fallout from the Hiroshima bomb would be increased over that of the global fallout by the additional movement occurring during the period from 1945 to the peak of global fallout release in the early 1960s, as this time period affects the Hiroshima bomb fallout but does not affect the global fallout.

Conclusion

Using the available data from Takeshita *et al.* (1976) on ^{137}Cs measured in soil cores from the Hiroshima area, it is possible to use spatial smoothing to discern a trend in the mean surface of the measured ^{137}Cs inventories. A major variable affecting the measured values can be reduced in its effect by careful modeling of local rainfall using detailed data available from the Japan Meteorological Agency. After this adjustment, there is no statistically significant evidence of any pattern of high measured values in any given area. While statistically non-significant patterns appear in geographical plots of the adjusted measurment data, the overall trend does not appear to correspond to a likely deposition of fallout from the Hiroshima bomb but rather to the influence of unmodeled or insufficiently modeled meteorological, hydrological, and geological variables. Unfortunately, much more detailed work would be necessary to estimate from these data, if it is even possible to properly estimate, the error probabilities, particularly false negative, for detecting a deposition of any particular size (i.e., maximum original areal deposition of ^{137}Cs in Bq m^{-2}) from the Hiroshima bomb in 1945, with available methods in spatial statistics. A better understanding of the reasons for the spatial variability of the measured values is needed. Full-depth cores with detailed sectioning could help to understand some important aspects of the movement of deposited ^{137}Cs in the soil environments where the existing samples were taken.

An important point to be emphasized here is that small numbers of additional measurements, even of very high quality, can contribute only very limited spatial information. Even in retrospect, adding the 1978 and later data to the 1976 data to attempt a combined spatial analysis would create as many problems as it would solve. It would create a large component of localized heterogeneity in the variability of the spatial process, which needs to be effectively modeled, and it would contribute little new spatial information because these later measurements are at locations identical to or very near the 1976 locations.

Generally speaking, there appears to be little to be gained from additional spatial modeling or analysis of the existing data that is based strictly on location. More work is needed in modeling the effects of variables that influence the environmental movement of global fallout and would have affected the environmental movement of any local fallout from the Hiroshima bomb. One potential avenue for global fallout is to investigate the effects of soil type and geomorphology, which probably do not depend too much on the exact locations of the 1976 samples of Takeshita *et al*. It would be a considerable advantage if the exact locations of the 1976 sampling could be more accurately determined and the sites investigated to accurately estimate variables such as terrain elevation, slope gradient and vegetation.

Acknowledgement

The Radiation Effects Research Foundation (RERF), Hiroshima and Nagasaki, Japan is a private, non-profit foundation funded by the Japanese Ministry of Health, Labour and Welfare (MHLW) and the U.S. Department of Energy (DOE), the latter in part through the National Academy of Sciences. This publication was supported by RERF Research Protocol RP #18-59. Special thanks is due to Sachiyo Funamoto of RERF for her help in organizing and extracting the relevant rainfall data from the AMeDAS CDs.

References

Anselin, L., 1995. Geographical Analysis 27, 93-115.

Aoyama, M., Hirose, K., Igarashi, Y., 2006. Re-construction and updating our understanding on the global weapons tests ^{137}Cs fallout. Journal of Environmental Monitoring 8, 431-438.

Bivand, R.S., Pebesma, E.J., Gomez-Rubio, V., 2008. Applied spatial data analysis with R. Springer, New York, NY.

Cressie, N.A.C., 1993. Statistics for spatial data (revised edn). John Wiley & Sons, New York, NY.

Cullings, H.M., Fujita, S., Hoshi, M., Egbert, S.D., Kerr ,G.D. Alignment and referencing of maps and aerial photographs. In: Young RW, Kerr GD (eds) Reassessment of the atomic bomb radiation dosimetry for Hiroshima and Nagasaki – Dosimetry System 2002. Hiroshima, Japan: Radiation Effects Research Foundation; 2005.pp.139-222. http://www.rerf.jp/shared/ds02/index.html Accessed 17 February 2011.

Cullings, H.M. A preliminary geospatial analysis of ^{137}Cs measured in soil cores from Hiroshima. In: Hoshi, M., Imanaka, T., eds, Current status of studies on radioactive fallout with “black rain” due to the Hiroshima atomic bomb. Hiroshima, Japan: Hiroshima City;2010.pp.121-136.

Daly, C., Neilson, R.P., Phillips, D.L., 1993. A statistical-topographic model for mapping climatological precipitation over mountainous terrain. Journal of Applied Meteorology 33, 140-158.

Garcia-Martino, A., Warner G.S., Scatena, F.N., Civco, D.L., 1996. Rainfall, runoff and elevation relationships in the Luquillo Mountains of Puerto Rico. Carribbean Journal of Science 32, 413-424.

Goovaerts, P., 2000. Geostatistical approaches for incorporating elevation into the spatial interpolation of rainfall. Journal of Hydrology 228, 113-129.

Goovaerts, P., Jacquez, G. M., 2004. Accounting for regional background and population size in the detection of spatial clusters and outliers using geostatistical filtering and spatial neutral models: the case of lung cancer in Long Island, New York. International Journal of Health Geographics 4, available at http://www.ij-healthgeographics.com/content/3/1/14. Accessed 5/24/2011.

Haiden ,T., Pistotnik, G., 2009. Intensity-dependent parameterization of elevation effects in precipitation analysis. Advances in Geosciences 20, 33-38.

Hashizume, T., Okajima, S., Kawamura, S., Takeshita, K., Tanaka, E., Nishimura, K., Tanaka, H., Maruyama, T., Yamada, H., Yoshizawa, T., 1978. Study on residual radioactivity in Hiroshima and Nagasaki. Journal of the Hiroshima Medical Association 31, 455-458.

He, Q., Walling, D.E., 1997. The distribution of fallout ^{137}Cs and ^{210}Pb in undisturbed and cultivated soils. Applied Radiation and Isotopes 48, 677-690.

Kawachi, T., Maruyama, T., Singh, V. P., 2001. Rainfall entropy for delineation of water resources zones in Japan. Journal of Hydrology 246, 36-44.
Kulldorff, M., 1997. A spatial scan statistic. Communications in Statistical Theory and Methods 26,1381-1496.
Kulldorff, M., Huang, L., Pickle, L., Duczmal, L., 2006. An elliptic spatial scan statistic. Statistics in Medicine 25:3929-3943.
Masuda, Y., 1989. Re-investigation about “black rain” after Hiroshima A-bomb. Tenki 36, 69-79.
Okajima, S., Fujita, S., Harley, J.H., Radiation doses from residual radioactivity. In: Roesch, W.C., ed, US-Japan joint reassessment of atomic bomb radiation dosimetry in Hiroshima and Nagasaki: Final Report. Hiroshima, Japan: Radiation Effects Research Foundation; 1987.pp.139-222. http://www.rerf.jp/shared/ds86/index.html Accessed 17 February 2011.
Patil, G.P., Joshi, S.W., Koli, R.E., 2010.PULSE, progressive upper level set scan statistic for geospatial hotspot detection. Environmental and Ecological Statistics 17, 149-182.
Sakaguchi, A., Kawai, K., Steier, P., Imanaka, T., Hoshi, M., Endo, S., Zhumadilov, K., Yamamoto, M., 2010. Feasibility of using ^{236}U to reconstruct close-in fallout deposition from the Hiroshima atomic bomb. Science of the Total Environment 408, 5392-5398.
Shizuma, K., Iwatani, K., Hasai, H., Hoshi, M., Oka, T., Okano, M., 1996. ^{137}Cs in soil samples from an early survey of Hiroshima atomic bomb and cumulative dose estimation from the fallout. Health Physics 71, 340-346.
Suzuki, H., 1962. Classification of Japanese climates. Geographical Review of Japan 35, 205-211 (in Japanese).
Takeshita, K., Sunayashiki, T., Takeoka, S., Kato, K. 1976. ^{137}Cs in soil of the black rain area northwest of the Hiroshima hypocenter. In: Hiroshima. Hiroshima, Japan: Research Institute for Nuclear Medicine and Biology, Hiroshima University; 1976. pp. 109-115.
Uda, M., Sugahara, Y., Kita, I. Meteorological conditions related to the atomic bomb explosion in Hiroshima. In: Collection of reports on investigations of the atomic bomb casualties. Tokyo, Japan: Science Council of Japan ; 1953. pp. 98-136.
United Nations Scientific Committee on the Effects of Atomic Radiation (UNSCEAR), 2000. Sources and Effects of Ionizing Radiation. United Nations, New York, NY.
Zhang, X., Long, Y., He, X., Fu, J., Zhang, Y., 2008. A simplified ^{137}Cs transport model for estimating erosion rates in undisturbed soil. Journal of Environmental Radioactivity 99, 1242-1246.

Appendix

Table 1 Measurement Data for ^{137}Cs in Soil

Nominal compass direction	Nominal distance km	X, km	Y, km	Elevation m	Inventory Bq m^{-2}
		Takeshita et al. (1976)			
N	3	0.165	2.893	4	1413
N	4	-0.564	4.181	18	2187
N	6	-0.169	5.947	121	1524
N	8	0.043	7.897	155	2916
N	10	-0.26	9.958	116	2945
N	12	-0.169	11.908	319	3056
N	14	0.074	13.821	237	5576
N	16	-0.108	16.176	203	2449
N	18	-0.048	18.015	233	4325
N	20	0.377	19.855	231	2512
N	22	0.165	21.915	281	1247
N	24	0.043	24.233	378	1439
N	26	0.195	26.183	379	2253
N	28	0.165	28.023	384	4755
N	30	0.226	30.415	585	3589
ENE	2	1.855	1.095	42	3001
ENE	4	3.442	1.91	58	2690
ENE	6	5.003	3.117	80	3090
ENE	8	6.429	4.552	137	3297
ENE	10	7.721	6.215	106	2945
ENE	12	9.012	7.487	155	3215
ENE	14	9.685	9.606	96	2971
ENE	16	10.977	11.139	130	3097
ENE	18	15.174	9.248	393	1617
ENE	20	13.775	14.042	378	3030
ENE	22	18.619	11.009	246	1010
ENE	24	20.448	11.857	272	1006
ENE	26	21.821	12.444	440	966
ENE	30	25.615	14.465	379	1417
ESE	2	1.72	-1.123	25	2882
ESE	4	2.689	-2.982	2	3944
ESE	6	5.192	-3.275	38	1532
ESE	8	6.645	-4.547	2	1358
ESE	10	8.555	-5.199	151	4544
ESE	12	10.143	-6.145	351	1813
ESE	14	12.215	-7.156	246	3086
ESE	16	13.641	-8.134	390	3193

Table 1 continued

Nominal compass direction	Nominal distance km	X, km	Y, km	Elevation m	Inventory Bq m^{-2}
ESE	18	15.228	-9.113	234	3541
ESE	20	17.031	-10.156	149	3452
ESE	22	18.78	-11.167	397	1672
ESE	24	20.448	-12.146	370	5206
ESE	26	22.467	-13.091	453	1983
ESE	28	23.704	-13.809	145	807
ESE	30	25.588	-15.081	51	1399
S	2	0.187	-2.232	2	1661
S	4	0.59	-3.569	2	1269
S	6	0.59	-5.852	17	2705
S	8	-1.132	-8.036	84	448
S	12	-0.136	-12.146	7	2094
S	14	-0.136	-14.07	37	2028
S	16	1.344	-16.385	9	1528
S	20	0.294	-19.744	99	796
S	22	-0.325	-21.733	67	3596
S	24	0.079	-23.429	40	1913
S	28	-0.782	-27.277	68	1180
WSW	16	-13.86	-8.102	83	1576
WSW	18	-15.582	-9.113	62	2298
WSW	20	-17.25	-10.058	131	2054
WSW	22	-19.268	-10.743	229	3230
WSW	24	-20.963	-11.95	277	5890
WSW	26	-22.309	-13.483	405	2956
WSW	28	-24.138	-14.07	502	2816
WSW	30	-25.618	-14.591	479	2875
W	4	-4.065	-0.177	42	2294
W	6	-6.083	0.312	189	1262
W	8	-7.994	0.019	39	1957
W	10	-10.039	0.019	66	2054
W	12	-11.895	0.051	377	2590
W	14	-13.913	0.084	443	1602
W	16	-15.905	0.051	585	2997
W	18	-17.761	0.019	516	2179
W	20	-19.914	0.051	417	3304
W	23	-22.605	0.997	536	936
W	25	-24.434	1.225	760	4965
W	27	-26.668	0.54	486	7086
W	30	-29.251	-0.992	415	1650
WNW	4	-3.473	1.877	88	1291

Table 1 continued

Nominal compass direction	Nominal distance km	X, km	Y, km	Elevation m	Inventory Bq m^{-2}
WNW	6	-5.357	3.345	69	2028
WNW	8	-6.836	4.258	152	1732
WNW	10	-8.801	4.682	318	2139
WNW	12	-9.42	6.769	338	947
WNW	14	-11.707	7.258	400	1406
WNW	16	-13.644	7.943	583	1062
WNW	18	-15.07	8.922	533	2250
WNW	20	-17.008	10.096	219	1421
WNW	22	-19.08	10.193	538	2538
WNW	24	-20.344	12.117	492	4499
WNW	26	-20.207	15.935	506	1443
WNW	28	-23.546	13.683	775	5384
WNW	30	-27.583	10.519	598	1602
WNW	32	-27.098	15.835	681	6819
NNW	2	-1.401	1.453	4	1384
NNW	4	-1.939	3.378	300	2727
NNW	6	-2.908	5.171	316	2098
NNW	8	-3.85	6.834	110	3175
NNW	10	-4.872	8.628	149	1536
NNW	12	-5.841	10.259	318	2087
NNW	14	-6.783	12.052	156	2997
NNW	16	-8.236	13.585	312	1839
NNW	18	-9.151	15.444	512	1106
NNW	24	-10.765	20.825	281	1069
NNW	20	-9.769	17.335	107	2634
NNW	22	-10.388	19.488	461	7311
NNW	26	-12.191	22.488	159	3108
NNW	28	-13.617	24.379	325	3963
NNW	30	-14.77	26.206	536	3182
		Hashizume et al. (1978)			
N	12	-0.109	12.468	130	3112
N	12	-0.088	12.589	150	1521
N	12	-0.029	12.555	155	4040
N	12	-0.045	12.49	170	2202
N	12	0.396	11.862	270	1865
N	12	0.207	11.706	320	3060
N	12	0.575	11.981	240	2176
N	12	0.156	12.433	190	1458
N	12	0.046	12.476	170	2538

Table 1 continued

Nominal compass direction	Nominal distance km	X, km	Y, km	Elevation m	Inventory Bq m^{-2}
N	12	-0.07	12.758	170	4166
N	12	-0.782	11.544	230	2253
N	14	-0.048	13.747	130	3367
N	14	-0.028	13.852	120	3323
N	14	0.032	13.783	190	1965
N	14	0.282	14.369	120	2479
N	14	-0.075	14.342	125	2257
N	14	0.149	13.944	140	2827
N	14	-0.298	13.544	130	2753
N	14	-0.476	13.744	290	2860
N	14	0.661	13.903	90	1854
N	14	0.598	14.335	120	3463
N	14	-0.57	14.423	120	4366
N	22	0.492	22.335	300	2039
N	22	0.434	22.333	300	2734
N	22	0.385	22.208	340	1695
N	22	0.479	22.213	300	1902
N	22	0.533	22.247	270	1203
N	22	-0.003	22.528	320	2005
N	22	0.374	22.48	340	2546
N	22	0.802	22.555	290	1795
N	22	0.798	21.291	260	1499
N	22	0.039	21.962	300	3922
N	22	-0.243	21.81	295	2568
NNW	14	-6.723	11.655	210	1839
NNW	14	-6.618	11.658	220	2327
NNW	14	-6.517	12.193	160	888
NNW	14	-6.785	12.153	165	3304
NNW	14	-7.748	12.029	280	3330
NNW	14	-7.908	11.904	250	1291
NNW	14	-7.283	12.603	560	4333
NNW	14	-7.521	12.577	520	2512
NNW	14	-7.714	12.175	325	4462
NNW	14	-6.395	12.827	280	2993
NNW	22	-11.161	19.309	320	4481
NNW	22	-10.731	19.519	390	4370
NNW	22	-10.664	19.836	410	3744
NNW	22	-11.096	19.051	270	2183
NNW	22	-11.027	19.121	320	1610
NNW	22	-10.496	18.872	320	4903

Table 1 continued

Nominal compass direction	Nominal distance km	X, km	Y, km	Elevation m	Inventory Bq m^{-2}
NNW	22	-10.567	18.643	270	3460
NNW	22	-10.535	20.029	490	3818
NNW	22	-11.4	19.587	490	2290
NNW	22	-11.189	20.036	220	2287
ESE	18	16.074	-8.496	260	3330
ESE	18	15.721	-8.618	260	1824
ESE	18	15.981	-8.624	240	3485
ESE	18	16.027	-8.748	230	2227
ESE	18	15.617	-8.65	265	2620
ESE	18	15.707	-8.774	230	2231
ESE	18	16.338	-8.232	205	1880
ESE	18	15.153	-8.68	315	2808
ESE	18	15.831	-8.049	220	2546
ESE	18	15.951	-8.477	230	1406
		Yamamoto et al. (1985)			
N	4	-0.564	4.181	18	2505
N	8	0.043	7.897	155	3367
N	10	-0.26	9.958	116	2616
NNW	6	-2.908	5.171	316	2601
NNW	10	-4.872	8.628	149	1532
NNW	12	-5.841	10.259	318	2190
NNW	16	-8.236	13.585	312	1339
NNW	22	-10.388	19.488	461	3164
NNW	24	-10.765	20.825	281	847
WNW	6	-5.357	3.345	69	2020
WNW	8	-6.836	4.258	152	2664
WNW	10	-8.801	4.682	318	3230
ESE	4	2.689	-2.982	2	4144
ESE	6	5.192	-3.275	38	1769
		Sakaguchi et al. (2010)			
N	10				3155
N	24				4092
N	28				2422
NNW	4				2808
NNW	8				5072
NNW	14				3235
WNW	10				1691